

# X-Ray Emission from the Galactic Supernova Remnant G12.0–0.1

Shigeo YAMAUCHI

*Department of Physics, Faculty of Science, Nara Women's University, Kitaoyanishi-machi, Nara 630-8506*  
yamauchi@cc.nara-wu.ac.jp

Aya BAMBA

*Department of Physics and Mathematics, Aoyama Gakuin University,*  
5-10-1 Fuchinobe, Chuo-ku, Sagamihara, Kanagawa 252-5258

and

Katsuji KOYAMA

*Department of Physics, Graduate School of Science, Kyoto University, Kitashirakawa-oiwake-cho, Sakyo-ku, Kyoto 606-8502*  
*Department of Earth and Space Science, Graduate School of Science, Osaka University,*  
1-1 Machikaneyama-cho, Toyonaka, Osaka 560-0043

(Received 0 0; accepted 0 0)

## Abstract

We present results of the Suzaku/XIS observation around the radio supernova remnant (SNR) G12.0–0.1. No significant diffuse emission extending in or along the radio shell was observed. Instead two compact X-ray sources, Suzaku J181205–1835 and Suzaku J181210–1842, were found in or near G12.0–0.1. Suzaku J181205–1835 is located at the northwest of the radio shell of G12.0–0.1. The X-ray profile is slightly extended over the point spread function of the Suzaku telescope. The X-ray spectrum has no line-like structure and is well represented by a power-law model with a photon index of 2.2 and an absorption column of  $N_{\text{H}}=4.9\times 10^{22}$  cm<sup>-2</sup>. The distances of Suzaku J181205–1835 and G12.0–0.1 are estimated from the absorption column and the  $\Sigma$ - $D$  relation, respectively, and are nearly the same with each other. These results suggest that Suzaku J181205–1835 is a candidate of a pulsar wind nebula associated with G12.0–0.1. From its location, Suzaku J181210–1842 would be unrelated object to G12.0–0.1. The X-ray profile is point-like and the spectrum is thin thermal emission with Fe K-lines at 6.4, 6.7, and 6.97 keV, similar to those of cataclysmic variables.

**Key words:** ISM: individual (G12.0–0.1) — ISM: supernova remnants — X-rays: individual (Suzaku J181205–1835 and Suzaku J181210–1842) — X-rays: spectra

## 1. Introduction

Supernovae remnants (SNRs) are main sites of heavy element production and of acceleration of high-energy particles in the Galaxy. X-rays are powerful tools to investigate the elements (abundances) by the plasma diagnostics and search for synchrotron X-rays from high-energy electrons. Although 273 Galactic SNRs have been discovered so far (Green 2009) by the radio, only limited fraction have been detected in the X-ray; X-ray properties of most of the SNRs have not been investigated yet. We have performed the Galactic plane survey project with ASCA (ASCA Galactic plane survey, AGPS, Yamauchi et al. 2002). AGPS covered the Galactic inner disk ( $|l| < 45^\circ$  and  $|b| < 0.4^\circ$ ) and the Galactic center region ( $|l| < 2^\circ$  and  $|b| < 2^\circ$ ) with successive pointing observations of about 10 ks exposure. AGPS detected X-ray emissions from  $\sim 30$  radio cataloged SNRs, in which 15 SNRs were new discoveries in the X-ray (Sugizaki et al. 2001; Sakano et al. 2002; Yamauchi et al. 2002). Among them, AGPS found an weak and diffuse X-ray source near G12.0–0.1, designated as AX J181211–1835 (Sugizaki et al. 2001). The X-ray spectrum of AX J181211–1835 was well represented by either a thin thermal emission or a power-law model

(Yamauchi et al. 2008). However, due to the poor photon statistics, the estimated parameters had large errors, and hence the origin of the X-ray was not well constrained.

Since Suzaku has a better spectral resolution, wider energy band, and lower/more stable intrinsic background than the previous X-ray satellites (Mitsuda et al. 2007), it is the suitable instrument to study a faint and diffuse sources. Based on the Suzaku data, Sezer et al. (2010) reported that the spectra of G12.0–0.1 were represented by a thermal emission+power-law model. Since G12.0–0.1 is a faint source at the Galactic Ridge, where a strong X-ray emission, called Galactic Ridge X-ray Emission (GRXE), is prevailing, the careful background subtraction is required. Thus, we reanalyzed the Suzaku data paying particular concern to background subtraction. In this paper, we report new results of the X-ray spectra and discuss the nature of G12.0–0.1.

## 2. Observations and Data Reduction

Suzaku observed the G12.0–0.1 region on 2007 October 2–3 with the X-ray CCD cameras (XIS) on the focal planes of the thin foil X-ray Telescopes (XRT). Details of Suzaku, XIS, and XRT are given in Mitsuda et al. (2007),

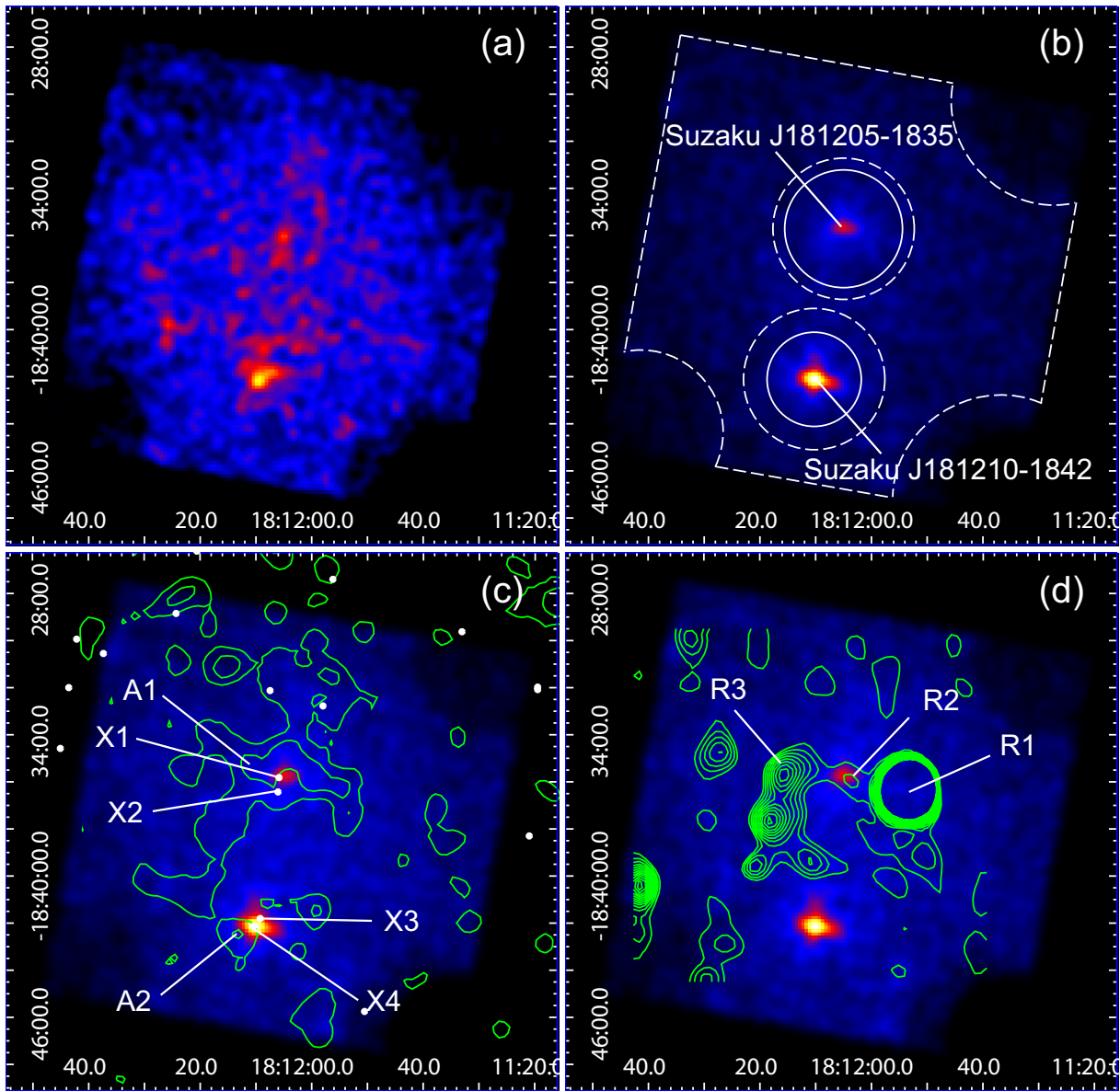


**Fig. 1.** XIS images in the (a) 0.7–2, (b) 2–8, and (c), (d) 0.7–8 keV smoothed with a Gaussian distribution of  $\sigma=24''$ . The coordinates are J2000.0. The data of XIS 0, 1, and 3 were co-added. Neither background subtraction nor vignetting correction is performed. The intensity levels of the X-ray and the radio bands are linearly spaced. The contour in (c) shows the ASCA GIS2+3 intensity map in the 0.7–10 keV smoothed with a Gaussian distribution of  $\sigma=60''$ , while the white dots show the positions of X-ray sources in the XMM-Serendipitous Source Catalog (Watson et al. 2009). A1 and A2 are the ASCA source named as AX J181211–1835 and AX J181213–1842, respectively, while X1, X2, X3, and X4 are XMM-Newton/Chandra sources named as 2XMM J181205.8–183549, 2XMM J181206.0–183625, 2XMM J181209.2–184149=CXO J181209.1–184146, and 2XMM J181210.5–184208=CXO J181210.3–184208, respectively. The contour in (d) shows the radio intensity map at 1.4 GHz using the NRAO VLA Sky Survey (NVSS) (Condon et al. 1998). R1, R2, R3 are G11.944–0.037, NVSS J181203–183558, and G12.0–0.1, respectively. The solid and dashed lines in (b) show source and background regions in the Suzaku analysis, respectively.

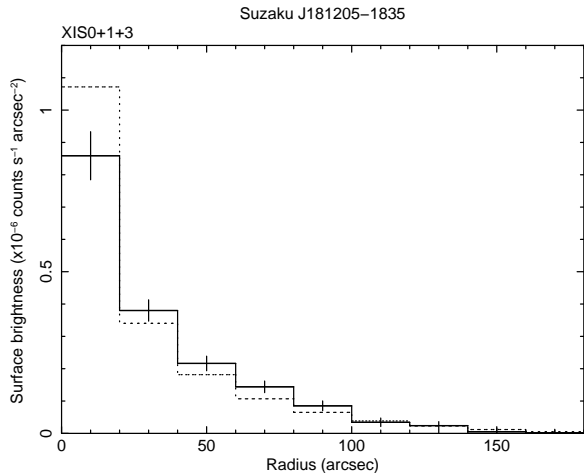


**Fig. 2.** Radial profile of Suzaku J181205–1835 (the solid line) in the 2–8 keV energy band and the best-fit PSF (the dotted line). The background counts estimated from an annulus region of  $180''$ – $210''$  radii were subtracted.

Koyama et al. (2007), and Serlemitsos et al. (2007), respectively. XIS sensor-1 (XIS 1) is a back-side illuminated CCD (BI), while the other three XIS sensors (XIS 0, 2, and 3) are front-side illuminated CCDs (FIs). The observed field was  $17'.8 \times 17'.8$  area with the center at  $(\alpha, \delta)_{J2000.0} = (273^\circ 02'08'', -18^\circ 6'25'')$ . Since one of the FIs (XIS2) turned dysfunctional in 2006 November, we used the data obtained with XIS 0, XIS 1, and XIS 3. The XIS was operated in the normal clocking mode with the time resolution of 8 s. The XIS employs the spaced-row charge injection (SCI) technique to rejuvenate the spectral resolution. Details concerning on the SCI technique are given in Nakajima et al. (2008) and Uchiyama et al. (2009).

Data reduction and analysis were made using the HEASoft version 6.11. The XIS pulse-height data for each X-ray event were converted to Pulse Invariant (PI) channels using the `xispi` software version 2009-02-28 and the calibration database version 2011-11-09. We excluded the data obtained at the South Atlantic Anomaly, during the earth occultation, and at the low elevation angle from the earth rim of  $< 5^\circ$  (night earth) and  $< 20^\circ$  (day earth). After removing hot and flickering pixels, we used the grade 0, 2, 3, 4, and 6 data. The resultant exposure time was 53.7 ks for each XIS detector.

### 3. Analysis and Results

#### 3.1. Image

Figure 1 shows X-ray images in the 0.7–2, 2–8, and 0.7–8 keV energy bands. The data of XIS 0, 1, and 3 were added to increase photon statistics. In the energy band above 2 keV (figure 1b), we see two compact X-ray sources. The north and the south sources have peaks at  $(\text{RA}, \text{Dec})_{J2000.0} = (18^{\text{h}}12^{\text{m}}05.0^{\text{s}}, -18^\circ 35'43'')$  and  $(\text{RA}, \text{Dec})_{J2000.0} = (18^{\text{h}}12^{\text{m}}10.3^{\text{s}}, -18^\circ 42'07'')$ , and hence we named them Suzaku J181205–1835 and Suzaku J181210–1842, respectively. The typical positional un-

certainty of Suzaku is  $19''$  (Uchiyama et al. 2008). In addition, the systematic error of the peak determination is  $8''$ .

#### 3.2. Suzaku J181205–1835

In the 0.7–8 keV band image of figure 1c, we show the ASCA intensity profile (the contour) and the peak position (labels A1 and A2), while the XMM-Newton/Chandra sources are displayed as X1, 2, 3, and 4. The error circle of Suzaku J181205–1835 includes 2XMM J181205.8–183549 (label X1) (the Second XMM-Newton Serendipitous Source Catalog Third Data Release: 2XMMi-DR3, Watson et al. 2009), and hence Suzaku J181205–1835 is identified with 2XMM J181205.8–183549. The nearest ASCA source is AX J181211–1835 (label A1) (the separation angle:  $\Delta\theta = 1'.58$ ). Since AX J181211–1835 is a faint source ( $5.4\sigma$  detection in the 0.7–7 keV band; Sugizaki et al. 2001) and is elongated to the east-west direction (see figure 1c), the uncertainty of the peak position would be large. Thus, Suzaku J181205–1835 and AX J181211–1835 are probably identical.

The radio intensity map at 1.4 GHz (Condon et al. 1998) is overlaid in the Suzaku image of figure 1d. A weak radio source NVSS J181203–183558 (label R2, NED; Condon et al. 1998) is near to Suzaku J181205–1835 ( $\Delta\theta = 23''$ ) and their error regions overlap each other. However, the separation angle between 2XMM J181205.8–183549 and NVSS J181203–183558 ( $\Delta\theta = 32''$ ) is larger than the positional errors of XMM-Newton ( $5''.22$  and systematic error =  $1''$ , 2XMMi-DR3) and NVSS ( $19''$ , NED). Thus, Suzaku J181205–1835 may not be identified with NVSS J181203–183558. We also searched for optical and infrared counterparts for Suzaku J181205–1835 by using the SIMBAD database and found no candidate.

Figure 2 shows the radial profiles in the 2–8 keV band, Suzaku J181205–1835 (the solid line) and the best-fit Point Spread Function (PSF, the dotted line) at the source position made using `xissim`. The background counts, estimated from an annulus region with radii of  $180''$ – $210''$ , were subtracted. A free parameter was a normalization of the PSF. The observed profile cannot be reproduced by the PSF with  $\chi^2/\text{d.o.f.} = 18.49/8 = 2.31$ ; it is slightly extended over the PSF. We note that 2XMM J181205.8–183549, an XMM-Newton counterpart, is also slightly extended ( $15''.7$ , 2XMMi-DR3).

X-ray spectra of Suzaku J181205–1835 were extracted from a  $2'.5$  radius circle (see figures 1 and 2). The background spectra were extracted from a source free region in the same FOV, as shown in figure 1b. We constructed the non-X-ray background (NXB) for the source and the background spectra from the night earth data using `xisnxbgen` (Tawa et al. 2008). After subtraction of the NXB from the source and the background spectra, we corrected the vignetting effect of the background spectra by the method shown by Hyodo et al. (2008) and subtracted the vignetting-corrected background spectra from the source spectra. The X-ray counts in the 1–10 keV energy band extracted from the source region were 1967,

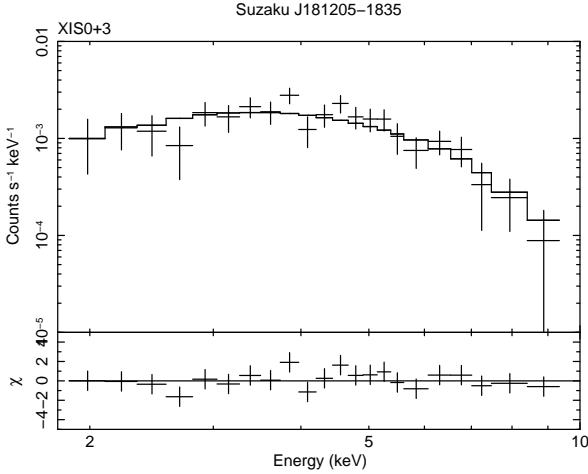


**Fig. 3.** X-ray spectrum of Suzaku J181205–1835 (XIS 0+3). The histogram shows the best-fit power-law model (see table 1).

**Table 1.** The best-fit parameters for the spectrum of Suzaku J181205–1835.\*

Parameter	Value
Model: power-law×absorption	
$N_{\text{H}}$ ( $\times 10^{22}$ cm $^{-2}$ )	$4.9^{+3.0}_{-2.3}$
$\Gamma$	$2.2^{+0.8}_{-0.7}$
$\chi^2/\text{d.o.f.}$	31.36/39
Flux $^\dagger$ ( $\times 10^{-13}$ erg s $^{-1}$ cm $^{-2}$ )	$3.0 \pm 0.4$

\* Errors are single parameter 90% confidence levels ( $\Delta\chi^2 < 2.7$ ).

$^\dagger$  Observed (absorbed) flux in the 2–10 keV energy band calculated from the best-fit model.

2625, and 1992 for XIS 0, 1, and 3, respectively, while after the background subtraction, the source counts were 467, 366, and 448, respectively. We co-added the XIS 0 and XIS 3 spectra, but treated the XIS 1 spectrum separately, because the response functions of the FIs and BI are different. Then, the background-subtracted spectra were grouped with a similar signal-to-noise ratio for a bin. Response files, Redistribution Matrix Files (RMFs) and Ancillary Response Files (ARFs), were made using `xisrmfgen` and `xissimarfgen`, respectively.

The background-subtracted spectrum is shown in figure 3. Only the FI CCD spectrum (XIS 0+3) is displayed for brevity. The X-ray spectra exhibit no emission line feature. We thus simultaneously fitted the XIS 0+3 and the XIS 1 spectra with a power-law model, modified by low-energy absorption. The cross sections of photoelectric absorption were taken from Balucinska-Church and McCammon (1992). This model can explain the spectra well with  $\chi^2/\text{d.o.f.} = 31.16/39 = 0.80$ . The best-fit parameters are listed in table 1, while the best-fit power-law model is shown in figure 3.

Since ASCA reported more extended emission (Yamauchi et al. 2008), we made Suzaku spectra within a  $4'.5$  circle from the source (the same size for the ASCA spectrum). The background spectra were extracted from the outer source free region in the same FOV. Then, the flux in the 2–10 keV band is  $(3.5 \pm 0.6) \times 10^{-13}$  erg s $^{-1}$  cm $^{-2}$ , nearly the same as that from the  $2'.5$  circle region (see table 1). Thus, we conclude that there is no largely extended non-thermal X-ray emission as reported with ASCA<sup>1</sup>.

We also examined possibility of largely extended thermal X-ray emission, by adding a thermal model with solar abundances (Anders & Grevesse 1989) (`apec` model in XSPEC) to the power-law function fixing the best-fit photon index and  $N_{\text{H}}$  value to those in table 1. We scanned the temperature range of 0.2–1 keV, and then obtained an upper limit of the thermal emission with  $kT < 1$  keV (absorbed) within a  $4'.5$  radius circle to be  $6 \times 10^{-14}$  erg s $^{-1}$  cm $^{-2}$  in the 2–10 keV band (90% confidence level).

We made timing data (X-ray counts/8 s) from a circle with a radius of  $1'.5$  centered on the peak position of Suzaku J181205–1835 for each detector and co-added the XIS 0, 1, and 3 data to maximize photon statistics. We found no significant intensity variation in the X-ray light curve. We also searched for a pulsation using `powspec`, but found no clear coherent pulsation in the range of 16–2048 s.

### 3.3. Suzaku J181210–1842

As shown in figure 1c, the position of the south source, Suzaku J181210–1842, well coincides with that of 2XMM J181210.5–184208=CXO J181210.3–184208 (label X4, Cackett et al. 2006; Evans et al. 2010; 2XMMi-DR3). The error circle of Suzaku J181210–1842 also overlaps with that of AX J181213–1842 ( $\Delta\theta = 0'.90$ ). Therefore, Suzaku J181210–1842 is identified with 2XMM J181210.5–184208=CXO J181210.3–184208=AX J181213–1842. No radio counterpart was found at the position of Suzaku J181210–1842 (figure 1d). On the other hand, 3 optical and infrared sources within the error region, USNO-B1.0 0712–00536743, 2MASS J18121061–184233, and SSTGLMC G0118947–00.1396, were found in the SIMBAD database.

Using the same method as that for Suzaku J181205–1835, we made a radial profile of Suzaku J181210–1842 and compared with the PSF. Figure 4 shows the radial profile of Suzaku J181210–1842 and the best-fit PSF. The observed profile is well fitted with the PSF ( $\chi^2/\text{d.o.f.} = 11.41/8 = 1.43$ ), and hence Suzaku J181210–1842 is a point source. We note that 2XMM J181210.5–184208, an XMM-Newton counterpart, is also a point source (2XMMi-DR3).

X-ray spectra of Suzaku J181210–1842 were extracted from a  $2'.0$  radius circle with the same background sub-

<sup>1</sup> We made the same analysis with no vignetting correction for the background spectra, and found that the flux is  $(8.0 \pm 0.8) \times 10^{-13}$  erg s $^{-1}$  cm $^{-2}$ , larger than that in table 1. Thus, we suspect that the ASCA extended emission is artifact caused mainly by an improper background subtraction (no vignetting correction).

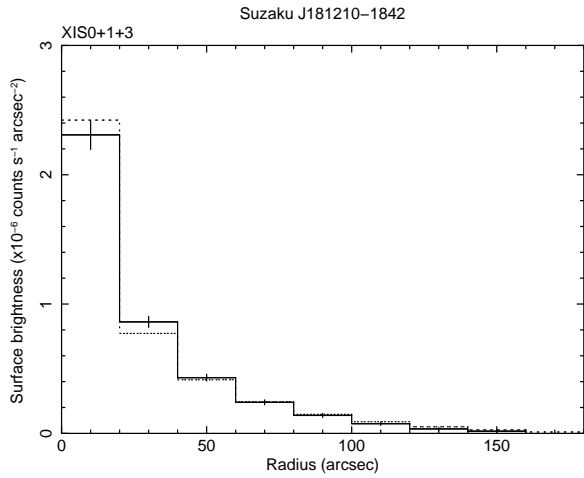


Fig. 4. Same as figure 2, but for Suzaku J181210–1842.

traction process as that for Suzaku J181205–1835. The X-ray counts from the source region in the 1–10 keV energy band were 1921, 2081, and 1660 for XIS 0, 1, and 3, respectively, while after the background subtraction the source counts were 969, 694, and 835, respectively. Then, the background-subtracted spectra were grouped as same as Suzaku J181205–1835.

Figure 5 shows the background-subtracted spectrum. Only the XIS 0+3 spectrum is displayed for brevity. We found a hump near the energy of Fe K-lines. We simultaneously fitted the XIS 0+3 and the XIS 1 spectra with a model consisting of thermal bremsstrahlung and a Gaussian line, and found a very broad line ( $\sigma \sim 230$  eV) leaving a wavy residual (the  $\chi^2$  value of 85.23 for d.o.f.=75). This suggests that the hump consists of several emission lines. Therefore, we next fitted the spectra adding three narrow Gaussian lines at 6.4, 6.7, and 6.97 keV to the thermal bremsstrahlung model. The center energies of the two lines were fixed at 6.4 and 6.97 keV. The fit was improved (the  $\chi^2$  value of 80.61 for d.o.f.=74). The best-fit parameters are listed in table 2 and the best-fit model is displayed in figure 5.

We extracted X-ray counts in the 1–8 keV band from a  $1'.5$  radius circle, co-added the XIS 0, 1, and 3 data, and examined time variation. No significant intensity variation was found in the X-ray light curve. We also searched for a pulsation but found no clear pulsation in the range of 16–2048 s.

#### 4. Discussion

Contrary to the ASCA result, Suzaku found neither thin thermal nor non-thermal X-rays extending largely in or along the radio shell of the SNR G12.0–0.1. Instead two compact X-ray sources, Suzaku J181205–1835 and Suzaku J181210–1842, were found in and near G12.0–0.1. Although these two sources have been already reported with XMM-Newton, the Suzaku observation provides more accurate spectra and more severe constraint. Here,

Table 2. The best-fit parameters for the spectrum of Suzaku J181210–1842.\*

Parameter	Value
Model: (bremsstrahlung+emission lines) $\times$ absorption	
$N_{\text{H}}$ ( $\times 10^{22}$ cm $^{-2}$ )	$3.4^{+0.8}_{-0.6}$
$kT$ (keV)	$>38$
$E_{\text{Line1}}^{\dagger}$ (keV)	6.4 (fixed)
$EW_{\text{Line1}}^{\ddagger}$ (eV)	$175 \pm 90$
$E_{\text{Line2}}^{\dagger}$ (keV)	$6.73^{+0.06}_{-0.05}$
$EW_{\text{Line2}}^{\ddagger}$ (eV)	$270 \pm 110$
$E_{\text{Line3}}^{\dagger}$ (keV)	6.97 (fixed)
$EW_{\text{Line3}}^{\ddagger}$ (eV)	$195 \pm 110$
$\chi^2/\text{d.o.f.}$	80.61/74
Flux $^{\S}$ ( $\times 10^{-13}$ erg s $^{-1}$ cm $^{-2}$ )	$8.7 \pm 0.5$

\* Errors are single parameter 90% confidence levels ( $\Delta\chi^2 < 2.7$ ).

$\dagger$  Energy of the emission line.

$\ddagger$  Equivalent width of the emission line.

$\S$  Observed (absorbed) flux in the 2–10 keV energy band calculated from the best-fit model.

we discuss the nature of these sources based on the Suzaku results.

##### 4.1. Suzaku J181205–1835

The Galactic HI column density ( $N_{\text{HI}}$ ) along the line-of-sight to Suzaku J181205–1835 is  $N_{\text{HI}}=2.0 \times 10^{22}$  cm $^{-2}$  (Dickey & Lockman 1990) or  $N_{\text{HI}}=1.4 \times 10^{22}$  cm $^{-2}$  (Kalberla et al. 2005). Using the CO intensity at the source position (164 K km s $^{-1}$ ; Dame et al. 2001) and the conversion factor to the  $N_{\text{H}_2}$  value ( $1.8 \times 10^{20}$  cm $^{-2}$  K $^{-1}$  km $^{-1}$  s; Dame et al. 2001), the Galactic H $_2$  column density ( $N_{\text{H}_2}$ ) is estimated to be  $N_{\text{H}_2}=3.0 \times 10^{22}$  cm $^{-2}$ . The total  $N_{\text{H}}$ ,  $N_{\text{H}}=N_{\text{HI}}+2N_{\text{H}_2}$ , is then  $(7.3\text{--}7.9) \times 10^{22}$  cm $^{-2}$ . The  $N_{\text{H}}=4.9 \times 10^{22}$  cm $^{-2}$  of Suzaku J181205–1835 is a bit larger than the half of the total  $N_{\text{H}}$  thorough the Galaxy. Therefore, Suzaku J181205–1835 would be in the Galactic inner disk at the distance of  $\sim 10$  kpc.

No reliable estimation, nor any report for the distance to G12.0–0.1 has been available so far. We therefore applied empirical relation between the surface brightness and the SNR diameter ( $\Sigma$ –D relation: e.g., Case & Bhattacharya 1998; Pavlović et al. 2013). Then the distance of G12.0–0.1 is calculated to be  $\sim 11$  kpc. Although the distance estimation methods for Suzaku J181205–1835 and G12.0–0.1 are the subject of large uncertainty, the distances of the two objects are roughly the same. We hence assume that Suzaku J181205–1835 is associated with SNR G12.0–0.1. In the following discussion, we assume the distance to Suzaku J181205–1835/G12.0–0.1 to be 10 kpc, with the reservation of a large error.

Suzaku J181205–1835 is spatially extended by sub-arcminute. The X-ray spectrum can be explained by a

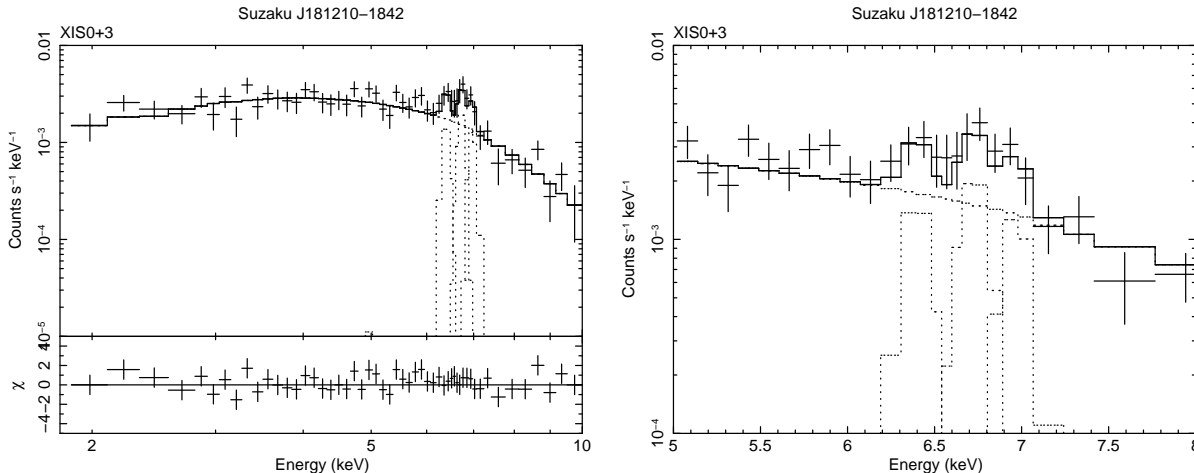


**Fig. 5.** Left: XIS spectrum (XIS 0+3) of Suzaku J181210–1842 (upper panel) and residuals from the best-fit model (lower panel). The histogram shows the best-fit bremsstrahlung + emission lines model (see table 2). Right: XIS spectrum (XIS 0+3) near the Fe-K energy (5–8 keV band). The histogram shows the best-fit model.

power-law model with a photon index of  $\Gamma=2.2^{+0.8}_{-0.7}$ , a typical value of SN 1006-like SNRs ( $\Gamma \sim 2.5$ –3, e.g., Koyama et al. 1995; Bamba et al. 2005) or pulsar wind nebulae (PWNe) ( $\Gamma \sim 2$ , e.g., Possenti et al. 2002; Kargaltsev & Pavlov 2008). No largely extended emission (power-law) near or around Suzaku J181205–1835 was found, which excludes possibility of SN 1006-like object.

The X-ray luminosity in the 2–10 keV band is calculated to be  $5.6 \times 10^{33}$  erg s $^{-1}$  at 10 kpc. Based on the empirical relation between an X-ray luminosity and a characteristic age of pulsars in PWNe (Possenti et al. 2002; Mattana et al. 2009), the age of Suzaku J181205–1835 is estimated to be  $\sim 3 \times 10^3$ – $3 \times 10^4$  yr. Middle-aged PWNe with characteristic ages of  $\sim 3 \times 10^3$ – $3 \times 10^4$  yr are expected to have small synchrotron nebulae with a size of  $\sim 2$ –10 pc (Bamba et al. 2010). This corresponds to  $0.7$ – $3.4$  at 10 kpc, in agreement with the extent of Suzaku J181205–1835 (figure 2).

In order to examine long-term intensity variation of Suzaku J181205–1835, we re-analyzed the ASCA spectrum from a  $3'$  radius circle after subtracting the background counts from an annulus region of  $3'$ – $6'$  radii. The flux is then  $(3.7 \pm 2.3) \times 10^{-13}$  erg s $^{-1}$  cm $^{-2}$  (2–10 keV), the same as the Suzaku result (see table 1). The X-ray flux of 2XMM J181205.8–183549 is estimated from the data of short exposure time (0.3–1.3 ks, 2XMMi-DR3). Although the values are different from detector to detector (MOS1, MOS2 and PN), they are in the range of  $(1.2$ – $21) \times 10^{-13}$  erg s $^{-1}$  cm $^{-2}$ . The Suzaku result ( $3.4 \times 10^{-13}$  erg s $^{-1}$  cm $^{-2}$  in the 2–12 keV band) is in this range. Thus, we conclude that there is no significant long-term intensity variation among the ASCA (1996), XMM-Newton (2003), and Suzaku (2007) observations.

These characteristics, the distance, non-thermal X-rays, reasonable extent, and no significant long-term intensity variation, suggest that Suzaku J181205–1835 is a new PWN candidate associated with SNR G12.0–0.1. The

thermal X-ray flux near or around this PMN candidate is less than 20% of the PWN flux, and hence G12.0–0.1 would be a PWN dominant SNR. If Suzaku J181205–1835 is a PWN, a fast rotation of a neutron star with a spin period less than 1 s would be expected. Since the XIS has no capability to detect such a fast rotation, we used the Hard X-ray Detector (HXD; Takahashi et al. 2007) data onboard Suzaku for the fast timing analysis with a  $61 \mu$ s time resolution and an accuracy of  $1.9 \times 10^{-9}$  s s $^{-1}$  per day (Terada et al. 2008). The resulting timing analysis in the 10–25 keV HXD data, however, showed no significant pulsation in the scanned period range of 10 ms to 1 s. Thus, future search for a pulsation in the radio and X-ray bands are encouraged.

Suzaku J181205–1835 has a large offset from the center of G12.0–0.1, which requires a very large projected velocity of  $\sim 1000$  km s $^{-1}$ . This value is near to a higher end of transverse velocities of radio pulsars (ATNF pulsar catalog<sup>2</sup>), and hence Suzaku J181205–1835 may have a bow-shock structure. Assuming that Suzaku J181205–1835 has the same wide band spectrum as Crab nebula, we can expect the total flux density of  $\sim 20$  mJy at 1 GHz. However, since Suzaku J181205–1835 has no clear radio counterpart (see section 3.2 and figure 1d) and the flux density of nearby radio source, NVSS J181203–183558, is  $\sim 5$  mJy at 1.4 GHz (Condon et al. 1998, NED), the flux density of Suzaku J181205–1835 would be less than 5 mJy. To reveal these issues, observations with high spatial resolution and high sensitivity in the radio and X-ray bands are also required.

#### 4.2. Suzaku J181210–1842

Judging from its location, Suzaku J181210–1842 would be unrelated object to G12.0–0.1. The X-ray lines at 6.4, 6.7, and 6.97 keV with the equivalent widths (EWs) of  $175 \pm 90$ ,  $270 \pm 110$ , and  $195 \pm 110$  eV, respec-

<sup>2</sup> <http://www.atnf.csiro.au/people/pulsar/psrcat/>

tively, are typical features of cataclysmic variables (CVs) (e.g., Hellier et al. 1998; Ezuka & Ishida 1999). Thus, Suzaku J181210–1842 is likely to be a CV although no clear coherent pulsation has not been found. The observed energy flux is similar to those observed with ASCA and XMM-Newton,  $(3\text{--}10)\times 10^{-13}$  erg s $^{-1}$  cm $^{-2}$  (Sugizaki et al. 2001; Cackett et al. 2006; 2XMMi-DR3).

This discovery of a new CV candidate on the Galactic plane means that there are many hidden CVs in the Galaxy. CV is proposed to be a prime candidate of the GRXE (e.g., Yuasa et al. 2012), because the GRXE spectra also exhibit three Fe K-lines at energies of 6.4, 6.7, and 6.97 keV (Ebisawa et al. 2008; Yamauchi et al. 2009). We find that the EW of the 6.4 keV line of Suzaku J181210–1842 is similar to GRXE ( $\sim 150$  eV), while that of the 6.7 keV line ( $\sim 200\text{--}300$  eV) is about a half of the GRXE (400–600 eV, e.g., Yamauchi et al. 2009; Uchiyama et al. 2013). This statement is true for most of the CVs, which are bright enough to measure the Fe K-lines (e.g., Ezuka & Ishida 1999). Thus, another population with a strong 6.7 keV line (EW > 400 eV at least) is required. Although active binary stars (ABs) are also proposed to be a potential candidate of the GRXE (Revnivtsev et al. 2009), the 6.7 keV line is too weak to explain the GRXE Fe K-line features (e.g., Tsuru et al. 1989; Mewe et al. 1997; Güdel et al. 1999). Thus, if the discrete source origin is applied, unresolved sources with a stronger Fe K-line than those of known bright CVs and ABs should exist.

The authors are grateful to all members of the Suzaku team. We thank Dr. Y. Terada for his useful comments. This research made use of the NASA/IPAC Extragalactic Database (NED) operated by Jet Propulsion Laboratory, California Institute of Technology, under contract with NASA and the SIMBAD database operated at the CDS, Strasbourg, France. This work is supported in part by the Grant-in-Aid for Scientific Research of the Ministry of Education, Science, Sports and Culture (SY, No. 21540234 and 24540232).

## References

- Anders, E., & Grevesse, N. 1989, *Geochim. Cosmochim. Acta*, 53, 197
- Balucinska-Church, M., & McCammon, D. 1992, *ApJ*, 400, 699
- Bamba, A., Yamazaki, R., Yoshida, T., Terasawa, T., & Koyama, K. 2005, *ApJ*, 621, 793
- Bamba, A., Anada, T., Dotani, T., Mori, K., Yamazaki, R., Ebisawa, K., & Vink, J. 2010, *ApJ*, 719, L116
- Cackett, E. M., Wijnands, R., & Remillard, R. 2006, *MNRAS*, 369, 1965
- Case, G. L., & Bhattacharya, D. 1998, *ApJ*, 504, 761
- Condon, J. J., Cotton, W. D., Greisen, E. W., Yin, Q. F., Perley, R. A., Taylor, G. B., & Broderick, J. J. 1998, *AJ*, 115, 1693
- Dame, T. M., Hartmann, Dap., & Thaddeus, P. 2001, *ApJ*, 547, 792
- Dickey, J. M., & Lockman, F. J. 1990, *ARA&A*, 28, 215
- Ebisawa, K., et al. 2008, *PASJ*, 60, S223
- Evans, I. N., et al. 2010, *ApJS*, 189, 37
- Ezuka, H., & Ishida, M. 1999, *ApJS*, 120, 277
- Green, D. A. 2009, *Bull. Astr. Soc. India*, 37, 45<sup>3</sup>
- Güdel, M., Linsky, J., Brown, A., & Nagase, F. 1999, *ApJ*, 511, 405
- Hellier, C., Mukai, K., & Osborne, J. P. 1998, *MNRAS*, 297, 526
- Hyodo, Y., Tsujimoto, M., Hamaguchi, K., Koyama, K., Kitamoto, S., Maeda, Y., Tsuboi, Y., & Ezoe, Y. 2008, *PASJ*, 60, S85
- Kalberla, P. M. W., Burton, W. B., Hartmann, Dap, Arnal, E. M., Bajaja, E., Morras, R., & Pöppel, W. G. L. 2005, *A&A*, 440, 775
- Kargaltsev, O., & Pavlov, G. G. 2008, 40 years of Pulsars: Millisecond Pulsars, Magnetars and More, AIP conference proceedings Vol.983, 171
- Koyama, K., Petre, R., Gotthelf, E. V., Hwang, U., Matsuura, M., Ozaki, M., & Holt, S. S. 1995, *Nature*, 378, 255
- Koyama, K., et al. 2007, *PASJ*, 59, S23
- Mattana, F., et al. 2009, *ApJ*, 694, 12
- Mewe, R., Kaastra, J. S., van den Oord, G. H. J., Vink, J., & Tawara, Y. 1997, *A&A*, 320, 147
- Mitsuda, K., et al. 2007, *PASJ*, 59, S1
- Nakajima, H., et al. 2008, *PASJ*, 60, S1
- Pavlović, M. Z., Urosëvić, D., Vukotić, B., Arbutina, B., & Göker, Ü. D. 2013, *ApJS*, 204, 4
- Possenti, A., Cerutti, R., Colpi, M., & Mereghetti, S. 2002, *A&A*, 387, 993
- Revnivtsev, M., Sazonov, S., Churazov, E., Forman, W., Vikhlinin, A., & Sunyaev, R. 2009, *Nature*, 458, 1142
- Sakano, M., Koyama, K., Murakami, H., Maeda, Y., & Yamauchi, S. 2002, *ApJS*, 138, 19
- Serlemitsos, P., et al. 2007, *PASJ*, 59, S9
- Sezer, A., Gök, F., Hudaverdi, M., Aktekin, E., & Ercan, E. N. 2010, *ASP Conference Series*, Vol.424, 171
- Sugizaki, M., Mitsuda, K., Kaneda, H., Matsuzaki, K., Yamauchi, S., & Koyama, K. *ApJS*, 2001, 134, 77
- Takahashi, T., et al. 2007, *PASJ*, 59, S35
- Tawa, N., et al. 2008, *PASJ*, 60, S11
- Terada, Y., et al. 2008, *PASJ*, 60, 25
- Tsuru, T. G., et al. 1989, *PASJ*, 41, 679
- Uchiyama, H., et al. 2009, *PASJ*, 61, S9
- Uchiyama, Y., et al. 2008, *PASJ*, 60, S35
- Uchiyama, H., Nobukawa, M., Tsuru, T. G., & Koyama, K. 2013, *PASJ*, 65, 19
- Watson, M. G., et al. 2009, *A&A*, 493, 339
- Yamauchi, S., et al. 2002, *Proc. of the IAU 8th Asian-Pacific Regional Meeting Vol.II (ASJ)*, p81
- Yamauchi, S., Ueno, M., Koyama, K., & Bamba, A. 2008, *PASJ*, 60, 1143
- Yamauchi, S., Ebisawa, K., Tanaka, Y., Koyama, K., Matsumoto, H., Yamasaki, N. Y., Takahashi, H., & Ezoe, Y. 2009, 61, S225
- Yuasa, T., Makishima, K., & Nakazawa, K. 2012, *ApJ*, 753, 129

<sup>3</sup> <http://www.mrao.cam.ac.uk/surveys/snrs/>